Revised Ms.: 2014BIOPHYSJ303585

SUPPORTING MATERIAL TO

CROWDING ACTIVATES ClpB AND ENHANCES ITS ASOCIATION WITH DnaK FOR EFFICIENT PROTEIN AGGREGATE REACTIVATION

Ianire Martín, Garbiñe Celaya, Carlos Alfonso, Fernando Moro, Germán Rivas and Arturo Muga

MATERIALS AND METHODS

Tracer sedimentation equilibrium (TSE): Data analysis.

The magnitude of the signal (S; absorbance at 650 nm) was followed as a function of the radial position (r). S_r is proportional to the total amount of protein and independent of the concentrations of all unlabeled species; this is particularly important in experiments done with Ficoll 70. For each solution composition, the radial dependence of the signal at sedimentation equilibrium was fitted to eqn. 1 to determine the whole-cell apparent signal-average buoyant molecular weight of wt- and ΔN-ClpB ($M^*_{i,app}$):

$$S_i(r) = S_i\ (r_0)\ \exp\left[\left(\frac{M^*_{i,app}}{2RT}\right)\left(r^2 - r_0^2\right)\right] \qquad \text{(eqn. 1)}$$

where S_i (r) is the magnitude of the signal (absorbance at 650 nm) proportional to the weight/volume concentration of wt- and ΔN-ClpB at radial position r; r_0 is an arbitrarily selected reference position; R is the molar gas constant; and T the temperature (1). The molecular weight analysis was done using the EQASSOC (2) and HETEROANALYSIS (3) programs, which yielded the same results within 5 % experimental error.

In the absence of Ficoll 70, all measurements meet conditions of thermodynamic ideality (high dilution of all macromolecular species) and therefore the apparent buoyant molecular weight experimental values ($M^*_{i,app}$) are equal to the actual buoyant molecular weights (M^*_i). The average molecular weight (M_i) of the different proteins can be obtained from the corresponding buoyant values with $M^*_i = M_i d_i$, where d_i denotes the specific density increments of wt- and ΔN-ClpB.

The experimental sedimentation equilibrium approach applied in this work, using short solution columns and low rotor speeds to yield shallow gradients, simplifies data analysis and interpretation. Under these conditions, $M^*_{i,app}$ becomes independent of radial distance and is well described by the solution average molecular weight value, which may be expressed as a function of the loading protein concentration and analyzed employing self-association relationships described elsewhere (4, 5). In this work, it has been assumed that wt- and ΔN-ClpB exist as an equilibrium mixture of monomers and hexamers with a thermodynamic equilibrium constant (K_6) given by

$$K_6 = \frac{w_6}{w_1^6} \qquad \text{(eqn. 2)}$$

where w_1 and w_6 denote the concentration (in weight/volume units) of monomers and hexamers, respectively. The average molecular weight is then given by

$$M_w = \frac{M_1(w_1 + 6w_6)}{w_{tot}} \qquad \text{(eqn. 3)}$$

where w_{tot} is the sum of the weight concentrations of monomers and hexamers. This model was then fit to the composition dependent average molecular weight data, $M^*_{i,app}$, obtained from eqn. 1 using a non-linear least squares procedures implemented in MATHLAB scripts (kindly provided by Dr. Allen Minton, NIH). This self-association scheme resulted to be the simplest one that globally described the SE data in the absence and presence of Ficoll 70 (see below) with a 95% confidence limit of statistical significance (6).

Non-ideal tracer sedimentation equilibrium analysis: The characterization of the corresponding SE measurements in the presence of Ficoll 70, in terms of association stoichiometry and equilibrium association constants, requires, as in the experiments done in the absence of crowder, to model the dependence of $M^*_{i,app}$ upon solution composition (7). It is also necessary to consider the effect that the interaction of the chaperone with all the species of the solution mixture might have on its apparent buoyant mass (4). The general expression that describes the condition of sedimentation equilibrium in a solution containing an arbitrary number of solute species at arbitrary concentrations is

$$M^*_{i,app} = M^*_i - \sum_j wj \left(\frac{d \ln \gamma_i}{dw_j} \right) M^*_{i,app} \qquad \text{(eqn. 4)}$$

where w_j denotes the w/v concentration of species j, and γ_i is the activity coefficient of species i. The quantity $(d\ln\gamma_i/dw_j)$ defines a thermodynamic magnitude measuring the free energy of interactions between species i and j, also referred to as thermodynamic interaction factor (5).

In a tracer SE experiment, the equilibrium concentration of the tracer protein (wt- and ΔN-ClpB) can be reliably measured independently of the gradients of the other solute components (Ficoll 70). Any effect of the unlabelled crowded species upon the signal gradient of the tracer will reflect either a net attractive or a net repulsive interaction between the tracer and the crowder. The quantitative analysis of the data would, in principle, require having a realistic model of excluded volume and other repulsive solute-solute interactions that may be relevant in concentrated and/or crowded solutions. In complex self-associating systems, as ClpB, this is extremely challenging. However, the analysis may be greatly simplified with the experimental design used in this study, which maintains constant the amount of the components present at high concentrations (Ficoll 70) that significantly contribute to the sum of the right-hand side of eqn. 4, and only changes the concentration of the dilute components (wt- and ΔN-ClpB). Under such conditions, the dependence of $M^*_{i,app}$ with the concentration of one or more dilute species may be directly modeled by eqn. 3 as in the absence of Ficoll 70 (for a more detailed description of this strategy see Rivas and Minton (8). Therefore, data in the presence of Ficoll can be analyzed without a previous knowledge of the

dependence of the activity coefficients of all species upon crowder concentration. The combined SE data for a given (single) crowder concentration (w_c) can be fitted by a self-association model that makes no assumptions on the non-specific interactions between dilute protein species (monomer and hexamers) and Ficoll 70. The non-linear modeling procedure then provides best-fit values of $M^*_{1,app}$, $M^*_{6,app}$ and K_6 for the concentration of Ficoll (w_c) at which the molecular weight values were determined.

SUPPORTING REFERENCES

1. Bocanegra, R., Alfonso, C., Rodriguez-Huete, A., Fuertes, M. A., Jimenez, M., Rivas, G. and Mateu, M. G. Association Equilibrium of the HIV-1 Capsid Protein in a Crowded Medium Reveals that Hexamerization during Capsid Assembly Requires a Functional C-Domain Dimerization Interface. 2013. *Biophys. J.* 884-893.

2. Minton, A.P. Modern Analytical Ultracentrifugation T.H. Schuster and T.H. Lave, editors. Birkhauser, Boston, MA, 1994, 81-93.

3. Cole, J.L. Analysis of heterogeneous interactions. 2004. *Methods Enzymol*. 384, 212-232.

4. Zorrilla, S., Jiménez, M., Lillo, P., Rivas, G. and Minton, A. P. General analysis of sedimentation equilibrium in highly nonideal solutions of associating solutes: application to ribonuclease. 2004. *Biophys. Chem.* 108, 89-100.

5. Rivas, G. and Minton, A. P. Beyond the second virial coefficient: Sedimentation equilibrium in highly non-ideal solutions. 2011. *Methods.* 54, 167-174.

6. Saroff, H.A. Evaluation of uncertainties parameters in binding studies: the sum-of-squares profile and Monte Carlo estimation. 1989. *Anal. Biochem.* 176, 161-169.

7. Rivas, G., Fernández, J. A. and Minton, A. P. Direct observation of the self-association of dilute proteins in the presence of inert macromolecules at high concentration via tracer sedimentation equilibrium: theory, experiment, and biological significance. 1999. *Biochemistry* 38, 9379-9388.

8. Rivas, G. and Minton, A. P. Non-ideal tracer sedimentation equilibrium: a powerful tool for the characterization of macromolecular interactions in crowder solutions. 2004. *J. Mol. Recognit.* 17, 362-367.

Figure S1

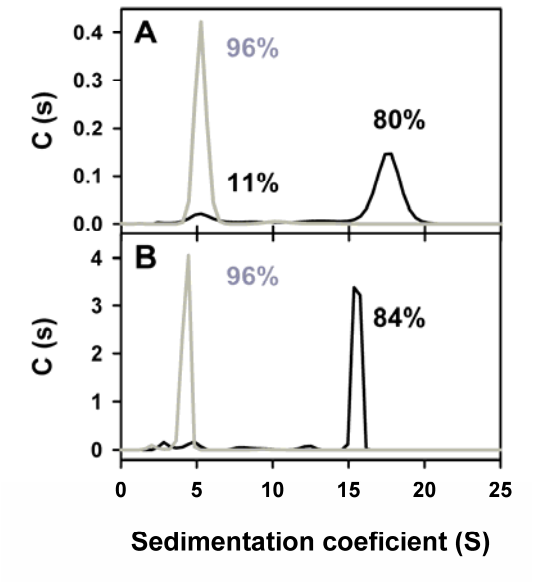

Figure S1. Effect of KCl on the sedimentation profile of wt ClpB and ΔN-ClpB. Sedimentation coefficient distributions of 10 µM (2 µM labeled with Alexa 647 and 8 µM unlabeled) wt ClpB (A) and ΔN-ClpB (B) at 50 mM Tris-HCl pH (7.5), 50 mM (black line) or 500 mM (grey line) KCl.

Figure S2

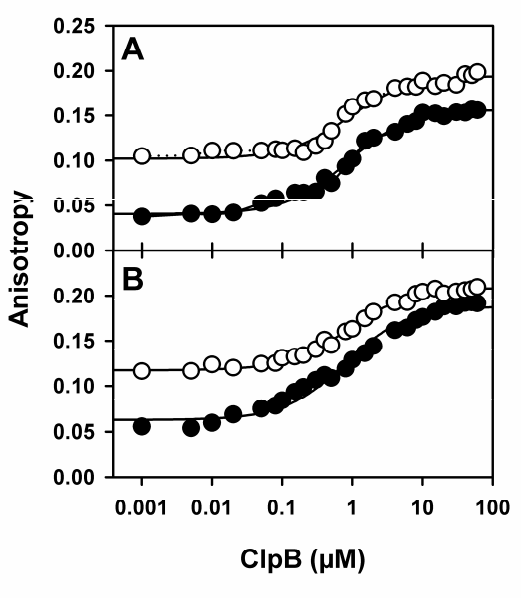

Figure S2. The affinity of the ATP-state of $ClpB_{trap}$ for substrates does not change in 15% (v/v) Ficoll 70. Fluorescence anisotropy of FITC-α-casein in the presence of increasing concentrations of (A) wt ClpB and (B) ΔN-ClpB in the absence (filled circles) and presence (empty circles) of 15 % Ficoll 70. Experimental data were fitted to a quadratic equation modeling a single binding site. Data are the mean ± SEM (n = 3).

Figure S3

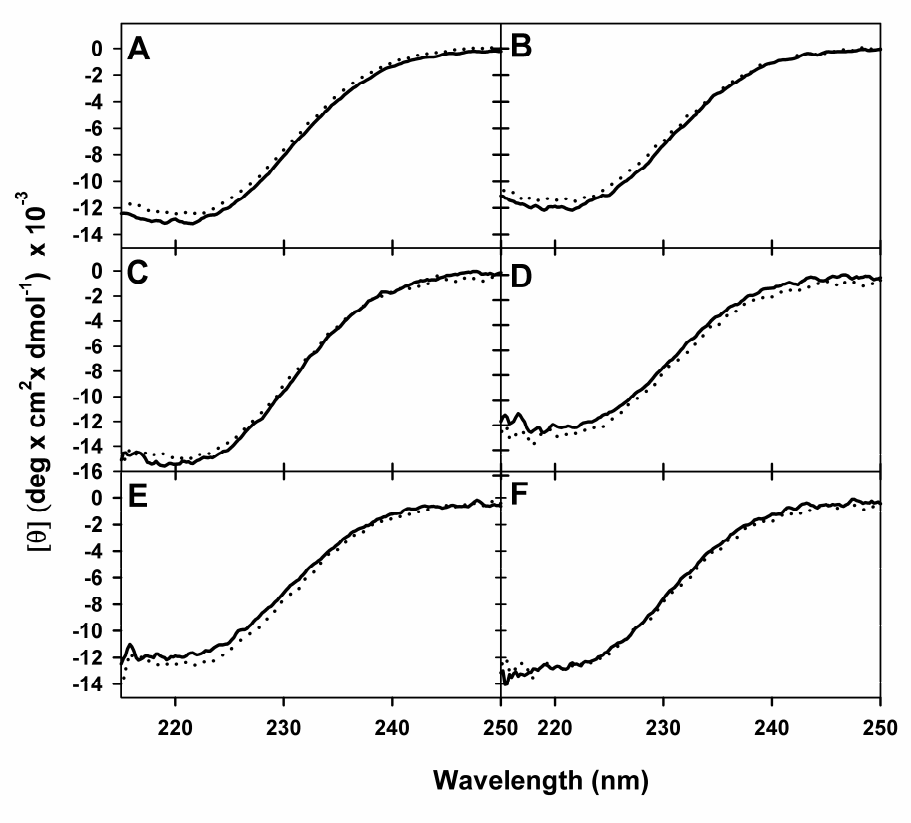

Figure S3. Secondary structure of ClpB under crowding. CD spectra of wt ClpB (A-C-E) and ΔN-ClpB (B-D-F) in apo- (A-B), ADP- (C-D) and $ATP_{(trap)}$-states (E-F) in the absence (solid line) and presence (dashed line) of 15 % Ficoll 70.

Figure S4

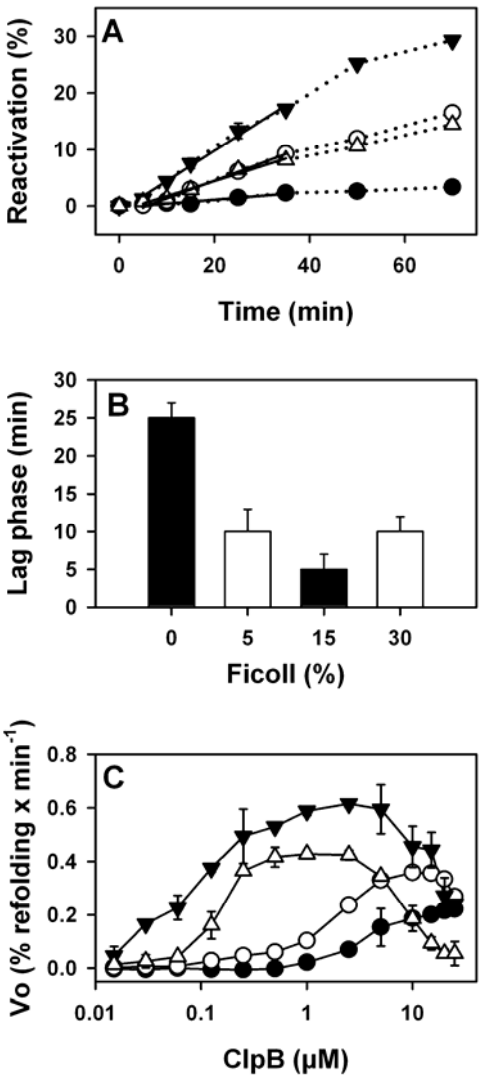

Figure S4. Effect of crowding on the reactivation of α-glucosidase aggregates at increasing ClpB concentrations. (A) Reactivation kinetics at 5 µM wt ClpB monomer in 0 % (filled circles), 5 % (empty circles), 15 % (filled triangles), and 30 % (empty triangles) Ficoll 70. (B) Disaggregation Lag phase at 5 µM wt ClpB monomer in 0 %, 5 %, 15 %, and 30 % Ficoll 70 (C) Initial reactivation rates at increasing ClpB concentrations measured under different crowding conditions. Same symbols as in (A). Values of the mean ± SEM from four independent experiments are shown.

Figure S5

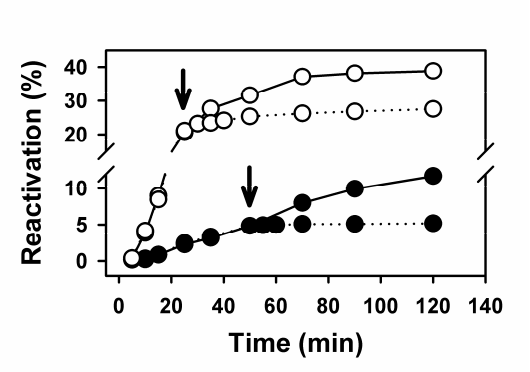

Figure S5. Subunit exchange takes place in the presence of crowder. Folding of G6PDH aggregates in buffer containing 50 mM KCl and 0 % (filled circles) or 15 % Ficoll 70 (empty circles). Experiments were carried out with 2.5 µM wt ClpB. The reactivation mixtures were divided in two aliquots and after recovery of a significant reactivation yield, buffer (solid line) or $ClpB_{trap}$ at 2.5 µM final concentration (dashed line) were added to each of them at the times indicated with black arrows.